Thrust of an Air-Augmented Waterjet

Robert G. Amos,* Glennon Maples,† and David F. Dyer‡
Auburn University, Auburn, Ala.

The waterjet is a marine propulsion device in which water is supplied to an internal pump that adds energy to the water and expels it aft at a high velocity. This investigation is concerned with the possibility of augmenting the thrust of a conventional waterjet by utilizing the energy of an expanding gas to impart additional momentum to the water stream. The device under study is one in which compressed air is injected into the high-pressure water stream leaving the water pump. A mixture of water and finely dispersed air bubbles is generated in a constant-area mixing chamber, which joins the water-pump outlet. The two-phase bubbly mixture enters the exhaust nozzle and expands under the action of a negative pressure gradient. Internal thrust is analytically determined under the restrictions of certain simplifying assumptions. The mixing process is analyzed through the use of a control volume encompassing the entire mixing chamber. The two-phase nozzle flow is analyzed through application of the conservation laws for a single air bubble and an incremental control volume over a nozzle section. Results indicate that thrust augmentation is possible and most effective for low pump-outlet pressures and/or high mass flow ratios in the range permitting bubbly flow. Thrust augmentation is found to be only weakly dependent on air-injection temperature.

Nomenclature

A = cross-sectional area
a = acoustic velocity
C_D = drag coefficient
C_p = specific heat at constant pressure
C_v = specific heat at constant volume
h_c = average convective heat-transfer coefficient
K = ratio of specific heats
k = thermal conductivity
L = exhaust-nozzle length
ℓ = radius of exhaust nozzle
M = Mach number
m = mass flow rate
Nu = Nusselt number
P = pressure
Pr = Prandtl number
Q = quality
R = gas constant
Re = Reynolds number
r = bubble radius
T = temperature
U = water velocity
V = air or bubble velocity
x = coordinate along nozzle center line
α = void fraction
β = nozzle half angle
μ = dynamic viscosity
ν = mass flow ratio
ρ = mass density
θ = thrust

Subscripts

a = ambient
c = air-plenum entrance
e = nozzle exit
f = properties evaluated at film temperature
g = air
i = pump outlet; mixing-chamber inlet
m = mixture
n = nozzle
o = mixing-chamber outlet; nozzle entrance
w = water
x = horizontal component of vector

Received February 28, 1972.
Index categories: Marine Propulsion; Multiphase Flows; Nozzle and Channel Flows.

*Graduate Assistant. Presently Project Engineer, Humble Oil Company, New Orleans, La.
†Associate Professor, Department of Mechanical Engineering. Member AIAA.
‡Associate Professor, Department of Mechanical Engineering.

Introduction

THE waterjet is a marine propulsion device in which water is supplied to an internal pump that adds energy to the water and expels it aft, through a nozzle, at a higher velocity than that of the incoming stream. Thrust is produced through the resulting momentum exchange.

The waterjet system is usually located within the hull of the craft and comprises three primary components: 1) an inlet system, which inducts water from outside the hull and directs it to the pump; 2) a power-driven pump, which adds energy to the water; and 3) an exhaust nozzle, through which the water is expelled aft, out of the hull. A typical arrangement of a waterjet unit installed in a boat is shown in Fig. 1.

This particular method of propulsion is not recent in development but is one of the oldest-known forms of mechanically propelling water craft. In 1661 a waterjet propulsion device was tested in England by Toogood and Hayes. This particular device consisted of a pump installed in a water channel which ran the full length of the boat.[1] James Rumsey, in 1787, demonstrated a boat utilizing this method of propulsion on the Potomac River.[2] Much experimental work on waterjets was carried on during the nineteenth century, and by 1900 the inherent disadvantages of propulsors of this type were well recognized. These disadvantages of high ducting losses and excessive weight rendered the waterjet system less attractive for general use than the more efficient, lightweight screw propeller system. However, the characteristics of good shallow and restricted water operation (made possible by the lack of external underwater appendages) and excellent maneuverability (accomplished by utilizing the propulsive mechanism for steering) maintained interest in waterjet propulsion for special-purpose application.[3]

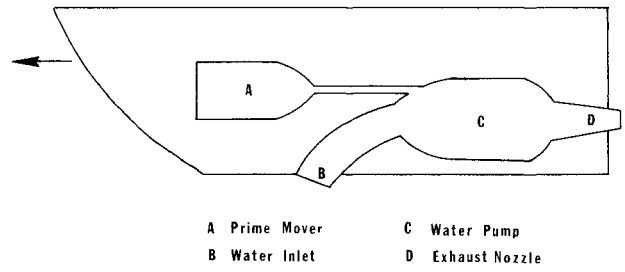

Fig. 1 Typical waterjet installation.

Recently, nonconventional ship designs have been developed in which little hull surface is exposed to the water. Exposing to the water less hull surface than that in older designs has resulted in a reduction of drag with a consequent allowance of increased ship speeds. The Captured-Air-Bubble Craft and the Hydrofoil Craft, both of which are nondisplacement ships, are illustrative of the new design trends. Each of these recently-developed ships is capable of cruise speeds up to 100 knots when matched with proper propulsive devices.[4-6] The search for favorable propulsors for these high-speed ships has concentrated primary attention on the waterjet system and the supercavitating propeller system.

At speeds in the 35-knot range, cavitation problems begin to deteriorate the efficiency of ordinary screw propellers to the extent that the efficiencies of the waterjet system and the screw propeller system become comparable.[7] With the development of the supercavitating propeller, the efficient speed range of the screw propeller has been extended to speeds in excess of 45 knots. However, the propulsive efficiency of the supercavitating propeller system is no greater than that of a well-designed waterjet system; and the former requires lengthy, expensive power trains which are not required on the latter.[7] The weight of the waterjet system, which includes the water in the pump and ducting, however, compares unfavorably with that of the supercavitating propeller system.

In considering the waterjet system for the propulsion of high-speed vessels, weight reduction becomes important if any useful payload is to result. Consequently, the application of lightweight aircraft-type turbojet and turbofan engines as prime movers for the waterjet pump has received increasing attention in recent years.

Prior theoretical and experimental efforts in the waterjet propulsion field have been concerned with problems including[6-15] 1) location of the propulsion system in a hull; 2) design of hull inlet for cavitation prevention; 3) design of system ducting for minimum friction losses; 4) design of lightweight pump and prime mover for satisfactory performance over the entire speed range; 5) design of water exhaust nozzle for minimum losses; and 6) matching of the individual components for efficient system operation.

This investigation is concerned with the possibility of augmenting the thrust of a conventional waterjet by utilizing the energy of an expanding gas, which may be supplied by the prime mover, to impart additional momentum to the water stream. A theoretical analysis is conducted of a system in which compressed air is injected into the high-pressure water stream leaving the waterjet pump.

Analytical Investigation

Problem Statement

The internal thrust produced by an air-augmented waterjet system, such as that depicted in Fig. 2, is to be determined analytically. Only constant-area mixing chambers and converging nozzles of the conical type are considered.

For the system under consideration, compressed air is injected perpendicularly into the high-pressure water stream leaving the waterjet pump; and a two-phase bubbly flow is generated in the mixing chamber. Upon completion of the mixing process, the two-phase mixture enters the exhaust nozzle and expands to an exit pressure which is equal either to the ambient pressure or to the pressure corresponding to mixture sonic velocity. The latter exit pressure, which is greater than the ambient pressure, is attained only for sufficiently large values of the ratio of nozzle inlet pressure to ambient pressure. In the exhaust nozzle, the gas bubbles, formed during the mixing process, expand under the action of the negative pressure gradient and do work on the water phase. The work done on the water phase by the expanding gas bubbles serves to increase the momentum of the water phase.

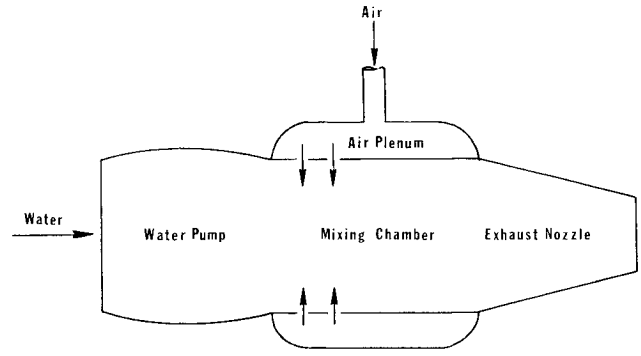

Fig. 2 Schematic diagram of air-augmented waterjet.

Assumptions

The solution of the problem at hand requires the determination of the physical parameters of a flowing two-phase mixture along the flow path. In order to achieve this end, a set of conservation equations is formulated under the restrictions of the following assumptions: 1) The flow is steady and quasi one-dimensional at the inlet and outlet of the mixing chamber and throughout the exhaust nozzle; 2) the mixing chamber and nozzle walls are frictionless and thermally nonconductive; 3) the water is incompressible and has a constant temperature throughout the system; 4) the air is a calorically perfect gas; 5) mass transfer between the gas and water phases is negligible; 6) air bubbles, formed during the mixing process, pass through the mixing-chamber outlet in the form of homogeneously dispersed spheres, each with a velocity equal to the water velocity; 7) the gas pressure in the air bubbles is at each point equal to the local water static pressure; 8) the air bubbles remain spherical during their residence in the nozzle, do not coalesce or divide, and have a constant value of their radii at any nozzle section; 9) in the exhaust nozzle, heat transfer takes place between the air bubbles and water only by the process of forced convection.

Governing Equations for Mixing Chamber

The physical processes occurring in the mixing chamber and exhaust nozzle are altogether dissimilar. Consequently, the analysis is most expeditiously conducted by considering each of these sections individually.

The following section gives the conservation equations for the mixing chamber. The behavior in the mixing chamber is complex. Compressed air is injected perpendicularly into the high-pressure water stream, and bubbles are formed some distance downstream of the injection point. A macroscopic approach, which avoids the highly nonequilibrium mixing region, is taken here.

The control volume shown in Fig. 3 is selected for this section of the analysis. The control surface "i" is chosen at a cross section slightly upstream of the point of air injection, and the control surface "o" is chosen far enough downstream that bubble formation is complete. Subject to the stated assumptions, the conservation equations for the control volume are readily developed.

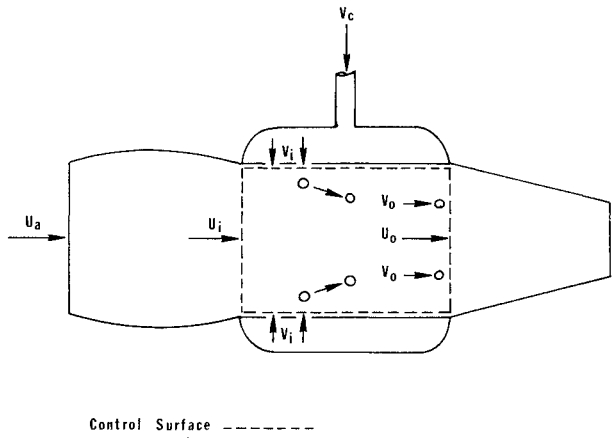

Fig. 3 Control volume for mixing-chamber analysis.

Conservation of water mass

The water mass flux at the control volume inlet and outlet, where the flow is steady and quasi-one-dimensional, is constant in the absence of phase change. Consequently,

$$\rho_w(1 - \alpha_o)A_oU_o = m_{wi} \tag{1}$$

Conservation of air mass

Through reasoning similar to that leading to Eq. (1), an air mass balance for the control volume yields

$$\rho_{go}\alpha_o A_o V_o = m_{gi} \tag{2}$$

Conservation of momentum

The only forces acting on the control volume are pressure forces; therefore, a horizontal momentum balance for the control volume requires that

$$P_{wi}A_i - P_oA_o = m_w(U_o - U_i) + m_gV_o \tag{3}$$

Conservation of energy

No heat or work crosses the control surfaces; hence, an energy balance for the control volume requires that

$$m_g[C_{Pg}T_{gi} + (1/2)V_i^2] + m_w[C_{Pw}T_w + (1/2)U_i^2] = m_g[C_{Pg}T_{go} + (1/2)V_o^2] + m_w[C_{Pw}T_w + (1/2)U_o^2] \tag{4}$$

Certain supporting equations, suggested by the previously enumerated assumptions, are used in conjunction with the conservation equations.

Air equation of state

The assumption that the air phase can be treated as a perfect gas allows the use of the ideal-gas equation of state:

$$P_o = \rho_{go}R_gT_{go} \tag{5}$$

Mixing-chamber exit velocity

The assumption that the air bubbles leave the mixing chamber with a velocity equal to that of the water specifies that

$$V_o = U_o \tag{6}$$

The preceding analysis was conducted without consideration of the bubble size at the mixing-chamber outlet. Any attempt to relate the bubble size to the void fraction necessarily requires the introduction of the number of bubbles as another variable and renders the resulting system of equations indeterminant.

A recourse to experimental endeavor indicates that little authoritative work has been done on the prediction of bubble sizes for bubbles formed in a manner similar to that under study. According to Wallis,[16] a gas jet leaving a single orifice into a stagnant fluid eventually breaks into individual bubbles having radii of approximately twice that of the orifice. For bubble formation in the presence of forced convection, the work by Hinze[17] illustrates the increased complexity of the problem.

In this analysis, a value for the radii of the bubbles leaving the mixing chamber is assumed. It is surmised that in practice the bubble size chosen can be attained by specification of the size of the inlet orifices. For a specified orifice size, a particular airflow rate can then be obtained through specification of the number of inlet orifices.

Governing Equations for Exhaust Nozzle

In early analyses of nozzle flows of two-phase gas-liquid mixtures, investigators, such as Tangren et al.[18] and Mottard and Shoemaker,[19] treated the flow as that of a homogeneous pseudofluid which obeyed the usual equations of single-component flow. The properties of the pseudofluid were determined on the basis of weighted averages of the properties of the individual phases; and phase velocity and temperature differences, which promote mutual momentum and heat transfer, were not considered.

Experimental studies, such as that conducted by Muir and Eichhorn,[20] have shown that the assumption of equal phase velocities for a two-phase flow under the action of strong pressure gradients is indeed a poor one. Consequently, in later analyses, such as that performed by Witte,[21] this homogeneous model has been abandoned in favor of the separated-flow model, which takes account of the fact that the two phases can have differing properties and velocities. The separated-flow approach is the one taken here for the analysis of the flow in the exhaust nozzle.

For a given pressure differential across a nozzle section, the air bubbles accelerate relative to the surrounding water since the inertia of a single air bubble is much less than that of the water surrounding it. The bubble conservation laws are most effectively developed from the viewpoint of an observer traveling with a bubble.

Bubble mass conservation

The neglect of mass-transfer effects and assumption of no bubble coalescence or division implies that

$$(D_g/Dt)[(4/3)\pi r^3\rho_g] = 0 \tag{7}$$

where, for the restriction of steady, one-dimensional flow, the derivative following the bubble is given as

$$(D_g/Dt)(\ \ ) = V(d/dx)(\ \ ) \tag{8}$$

Bubble momentum conservation

As the bubble moves through the nozzle, its progress is impeded by a drag force and an added-mass effect. The drag force is a function of the velocity of the bubble relative to the surrounding water, and the added-mass effect is dependent upon the bubble's acceleration relative to the neighboring fluid. Subject to the previously stated assumptions, a balance of the horizontal component of mo-

mentum for the bubble yields

$$\frac{2}{3}\pi r^3\rho_w\left(\frac{D_g}{Dt}V - \frac{D_w}{Dt}U\right) + \frac{4}{3}\pi r^3\rho_g\frac{D_g}{Dt}V + C_D\frac{1}{2}\rho_w\pi r^2(V-U)|V-U| + \frac{4}{3}\pi r^3\frac{dP}{dx} = 0 \quad (9)$$

where, for the restriction of steady, one-dimensional flow, the derivative following a water element in juxtaposition with the bubble is given as

$$(D_w/Dt)(\ ) = U(d/dx)(\ ) \quad (10)$$

The absolute value in Eq. (9) assures that the drag force acts in a direction opoosed to that of the bubble movement.

Bubble energy conservation

With the additional assumption that viscous dissipation is negligible, a bubble energy balance requires that

$$4\pi r^2h_c(T_g - T_w) + C_{vg}\frac{D_g}{Dt}\left(\frac{4}{3}\pi r^3\rho_gT_g\right) + P\frac{D_g}{Dt}\left(\frac{4}{3}\pi r^3\right) = 0 \quad (11)$$

In order to complete the formulation of the basic equations governing the exhaust-nozzle flow, attention is now directed to the incremental control volume shown in Fig. 4. Neglecting differentials of order higher than one, the conservation laws, subject to the pertaining assumptions, are readily developed for the incremental control volume.

Conservation of air mass

$$(d/dx)(\rho_g\alpha A_nV) = 0 \quad (12)$$

Conservation of water mass

$$(d/dx)[\rho_w(1-\alpha)A_nU] = 0 \quad (13)$$

Conservation of horizontal component of momentum

$$(dP/dx) + \rho_w(1-\alpha)UdU/dx + \rho_g\alpha VdV/dx = 0 \quad (14)$$

Certain supporting equations are used in conjunction with the previous conservation equations.

Air equation of state

The assumption that the air phase can be treated as a perfect gas allows the use of the ideal-gas equation of state:

$$P = \rho_gR_gT_g \quad (15)$$

Nozzle geometry

The exhaust nozzle is converging and has a conical shape. At any nozzle section x, the nozzle cross-sectional area is given by

$$A_n(x) = \pi(l_0^2 - 2xl_0\tan\beta + x^2\tan^2\beta) \quad (16)$$

Bubble heat-transfer coefficient

The heat transfer between a single bubble and the surrounding water is assumed to be analagous to that occurring between a stationary, solid sphere immersed in a water stream which is flowing with a velocity equal to the bubble relative velocity at the nozzle section in question. Effects of free convection are considered negligible in comparison to the effects of forced convection.

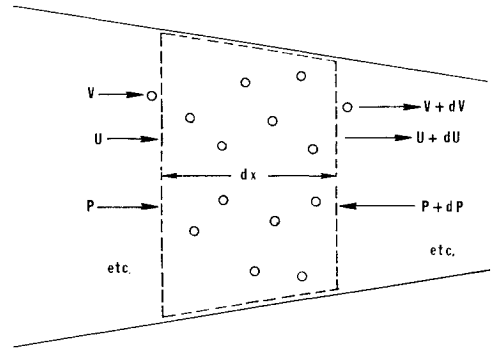

Fig. 4 Control volume for exhaust-nozzle analysis.

The heat-transfer coefficient is determined from an empirical relation developed by Vliet and Leppert[22] for forced convection heat transfer from an isothermal sphere to water. This relation, which is applicable in the Reynolds number range $1 < Re < 3 \times 10^5$, is

$$Nu \cdot Pr^{-0.3}(\mu_w/\mu_f)^{0.25} = 1.2 + 0.53 \cdot Re^{0.54} \quad (17)$$

where

$$Nu = h_c2r/k_w \quad (18)$$

and

$$Re = \rho_w2r(V-U)/\mu_w \quad (19)$$

Bubble drag coefficient

For low Reynolds numbers, the bubble drag coefficient is taken as that for a solid sphere moving with the bubble relative velocity. The drag coefficient relations and the Reynolds number ranges in which they are applied are as follows:

$$C_D = (24/Re)[1 + (3/16)Re] \text{ for } Re \leq 2 \quad (20)$$

and

$$C_D = 18.5/Re^{0.6} \text{ for } 2 < Re \leq 500 \quad (21)$$

where, by definition,

$$C_D = \text{Drag}/\frac{1}{2}\rho_w(V-U)^2\pi r^2 \quad (22)$$

Equation (20) is Oseen's improvement of Stokes' solution as given in Ref. 23, and Eq. (21) is an empirical relation presented in Ref. 24.

For the higher Reynolds number range, results of experiments involving air bubbles rising in vertical water columns have been presented by Haberman and Morton.[25] These results indicate a divergence in the bubble drag coefficient and the solid-sphere drag coefficient. On the basis of Haberman and Morton's results, the following drag coefficients are used in this analysis in the Reynolds number ranges indicated:

$$C_D = 1.0 \text{ for } 500 < Re \leq 1000 \quad (23)$$

and

$$C_D = 2.5 \text{ for } 1000 < Re \quad (24)$$

Equation (23) represents an average of Haberman and Morton's results in the specified Reynolds number range, and Eq. (24) is in actual agreement with those results.

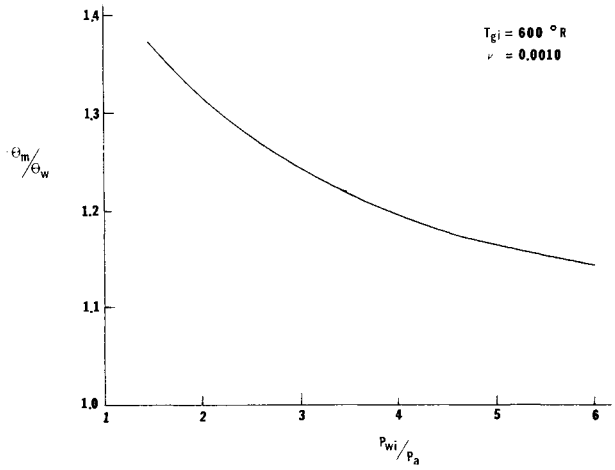

Fig. 5 Variation of thrust augmentation with pump-outlet pressure.

Compressibility effects

Liquids are seldom accelerated to velocities at which compressibility effects become important. However, for a two-phase gas-liquid mixture, the mixture sonic velocity may be considerably below that of either component; and compressibility effects may become important. Gouse and Brown[26] report sonic velocities in homogeneous air-water mixtures at values of approximately 10% of that for the gas phase alone when ratios of air mass to water mass are in the range of 10^{-4}–10^{-2}. Muir and Eichhorn[20] have experimentally verified the compressibility phenomena of choking in a two-phase air-water nozzle flow for mixture average velocities on the order of 70 fps at the nozzle throat.

The expression for mixture sonic velocity employed here is one analytically determined by Henry et al.[27] for a two-phase mixture at rest and is

$$a_m^2 = [(1-Q)\rho_g + Q\rho_w]^2/[\frac{Q\cdot\rho_w^2}{a_g^2} + \frac{(1-Q)\cdot\rho_g^2}{a_w^2}] \quad (25)$$

The mixture local Mach number is defined on the basis of a weighted average of the air and water velocities as

$$M_m = a_m/[(1-\alpha)U + \alpha V] \quad (26)$$

Governing Thrust Equation

The internal thrust developed by the waterjet system when operating at a velocity U_a is given by

$$\Theta = m_w(U_e - U_a) + m_g V_e + A_e(P_e - P_a) \quad (27)$$

Use of this eouation implies that there is no external acceleration or deceleration of the water stream.

Solution Technique

The mixing process is described by Eqs. (1–6). For given pump-outlet and air-injection conditions along with a specified mixing-chamber geometry, this set of six equations is readily solved for the parameters: U_o, V_o, α_o, ρ_{go}, T_{go}, and P_o. These six parameters and the assumed value for r_o completely specify conditions at the exhaust-nozzle entrance.

The equations describing the nozzle flow may be manipulated to form the following set:

$$\frac{K}{K-1}PV\frac{dr}{dx} + \frac{1}{K-1}\frac{rV}{3}\frac{dP}{dx} + h_c(T_g - T_w) = 0 \quad (28)$$

$$\frac{dP}{dx} + (\rho_g + \frac{\rho_w}{2})V\frac{dV}{dx} - \frac{\rho_w U}{2}\frac{dU}{dx} + \frac{C_D 3\rho_w}{8r}(V-U)|V-U| = 0 \quad (29)$$

$$(1-\alpha)\rho_w U\frac{dU}{dx} + \rho_g\alpha V\frac{dV}{dx} + \frac{dP}{dx} = 0 \quad (30)$$

$$\frac{1}{A}\frac{dA}{dx} + \frac{1}{U}\frac{dU}{dx} - \frac{1}{1-\alpha}\frac{d\alpha}{dx} = 0 \quad (31)$$

$$\frac{1}{A}\frac{dA}{dx} + \frac{1}{V}\frac{dV}{dx} + \frac{1}{\alpha}\frac{d\alpha}{dx} + \frac{1}{\rho_g}\frac{d\rho_g}{dx} = 0 \quad (32)$$

$$\frac{1}{\rho_g}\frac{d\rho_g}{dx} + \frac{3}{r}\frac{dr}{dx} = 0 \quad (33)$$

and

$$\frac{dP}{dx} - \rho_g R_g\frac{dT_g}{dx} - T_g R_g\frac{d\rho_g}{dx} = 0 \quad (34)$$

For the above equations, A is given by Eq. (16); h_c is given by Eq. (17); and C_D is given by the applicable equation from the group: (20), (21), (23), and (24). With the substitution of the relations for A, h_c, and C_D, Eqs. (28–34) form a system of seven nonlinear, coupled, first-order differential equations in the independent variable x and the seven dependent variables: U, V, P, T_g, α, ρ_g, and r. The system is, in principle, capable of solution.

The Euler-Cauchy method[28] is used with the system of Eqs. (28–34) in order to determine the flow parameters as functions of the distance along the axis of the nozzle. At the nozzle section $x = 0$, the boundary values determined in the first section of the analysis along with a specified nozzle half-angle allow solution of Eqs. (28–34) for the values of the derivatives at $x = 0$. The values of the dependent variables, an incremental distance Δx downstream of $x = 0$, are calculated by relations of the form

$$V_{x+\Delta x} = V_x + \frac{dV}{dx}\Big|_x \Delta x \quad (35)$$

This process is repeated stepwise for a specified Δx until a nozzle pressure corresponding to the ambient pressure or a Mach number of unity is reached. The size of the increment used is determined by carrying out the procedure for various values of Δx and comparing the resulting values of the dependent variables at the nozzle exit. An increment Δx is considered satisfactory when further reductions in its value effect the nozzle-exit parameters by less than 1%. This calculative procedure was executed with an IBM 360 Computer.

With the values: U_e, V_e, and P_e, Eq. (27) is used to determine the waterjet thrust.

Results and Discussion

The case of a small air-augmented waterjet, operating at a velocity of 20 fps, is analyzed for varying pump-outlet

Table 1 Two-phase thrust and associated nozzle lengths for various pump-outlet pressures; T_{gi} = 600°R, ν = 0.0010

Pump-outlet pressure, lbf/ft²	Thrust, lbf	Nozzle length, ft
3180	21.6	0.053
4240	34.6	0.113
5300	44.0	0.144
6360	51.7	0.166
8480	64.3	0.195
10600	74.7	0.216
12720	83.8	0.231

Table 2 Two-phase thrust and associated nozzle lengths for various mass flow ratios; P_{wi} = 4240 lbf/ft², T_{gi} = 600°R

Mass flow ratio	Thrust, lbf	Nozzle length, ft
0.00025	28.5	0.158
0.00050	30.7	0.141
0.00100	34.6	0.113
0.00150	38.1	0.088

and air-injection conditions. Specified quantities are as follows:

l_o (ft) = 0.0833
P_a (lbf/ft²) = 2120
P_{wi} (lbf/ft²) = 3180; 4240; 5300; 6360; 8480; 10600; 12720
r_o (ft) = 0.00025
T_{gi} (°R) = 530; 600; 800; 900
T_w (°R) = 530
U_a (ft/sec) = 20
U_i (ft/sec) = 20
V_i (ft/sec) = 40
β (deg.) = 10
ν . . . = 0.00025; 0.0005; 0.0010; 0.0015

For an air-injection temperature of 600°R and a mass flow ratio of 0.0010, the two-phase thrust and associated nozzle lengths are presented for the various pump-outlet pressures in Table 1. The thrust increases with increasing pump-outlet pressure. With the pump-outlet pressures exceeding 5300 lb/ft², the exhaust nozzles are operating under choked conditions; hence, the indicated two-phase thrust values for this pressure range are not the maximum attainable values. The maximum thrust for the choked nozzles may be achieved by allowing the flow expansion to continue through a diverging nozzle section.

The ratio of augmented thrust to the thrust developed by a conventional waterjet, operating under conditions similar to those considered here, is shown as a function of the ratio of pump-outlet pressure to ambient pressure in Fig. 5. Greatest thrust augmentation is seen to occur at the lower pressure ratios. As the pressure ratio is decreased toward unity, the nonaugmented thrust approaches a value of zero; and the two-phase thrust approaches the small, but nonzero, value of the thrust due to the air alone. Therefore, the thrust ratio is expected to increase asymptotically as the pressure ratio is decreased toward unity. With increasing pump-outlet pressure, the void fraction at the mixing-chamber outlet decreases; and since the size of the bubbles at this point remains fixed at the specified value, the number of bubbles available to perform work on the water phase decreases. The decrease in the number of air bubbles results in the two-phase thrust approaching the nonaugmented value for increasing pressure ratio.

An indication of the effectiveness of the momentum transfer from the gas phase to the water is given in Fig. 6.

Table 3 Two-phase thrust and associated nozzle lengths for various air-injection temperatures: P_{wi} = 4240 lbf/ft², ν = 0.0010

Air-injection temperature, °R	Thrust, lbf	Nozzle length, ft
530	34.6	0.113
600	34.6	0.113
800	34.9	0.110
900	35.2	0.107

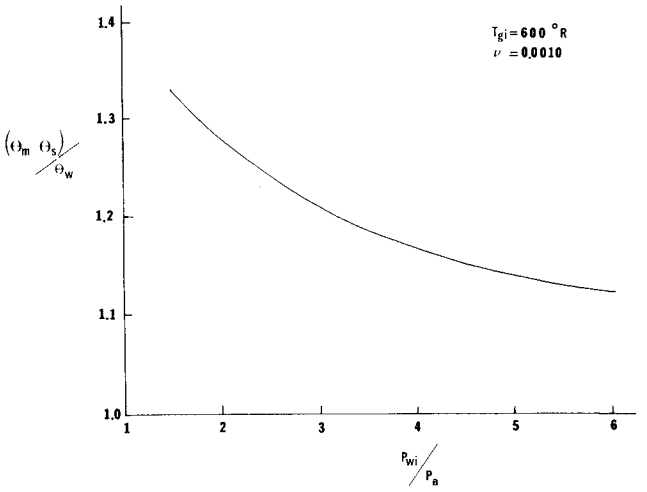

Fig. 6 Difference in the two-phase thrust and the thrust available from the air alone.

The difference in the two-phase thrust and that available from the air alone is seen to be greater than the nonaugmented thrust for all pressure ratios considered. Thrust of the air alone is determined by assuming that air with a flow rate of that used in the two-phase device expands isentropically from the pump-outlet pressure to the ambient pressure.

For a pump-outlet pressure of 4240 lb/ft² and an air-injection temperature of 600°, the values of two-phase thrust and associated nozzle lengths are presented for various mass flow ratios in Table 2. Thrust increases with increasing mass flow ratio. The ratio of two-phase thrust to nonaugmented thrust is shown as a function of mass flow ratio in Fig. 7. The thrust ratio approaches a value of unity as the mass flow ratio decreases toward zero. This behavior is anticipated since a mass flow ratio of zero corresponds to the flow of water alone. Increasing the mass flow ratio results in an increase in the void fraction at the mixing-chamber exit and a consequent increase in the number of bubbles available to perform work on the water; consequently, thrust increases with increasing mass flow ratio. The analysis is not carried to higher mass flow ratios since, under the specified conditions of pressure and temperature, void fractions greater than those commonly associated with bubbly flow would be attained.

The two-phase thrust and associated nozzle lengths are presented in Table 3 for a pump-outlet pressure of 4240

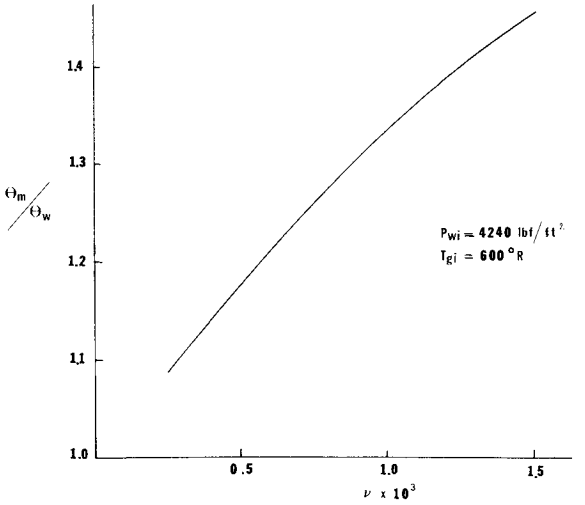

Fig. 7 Variation of thrust augmentation with mass flow ratio.

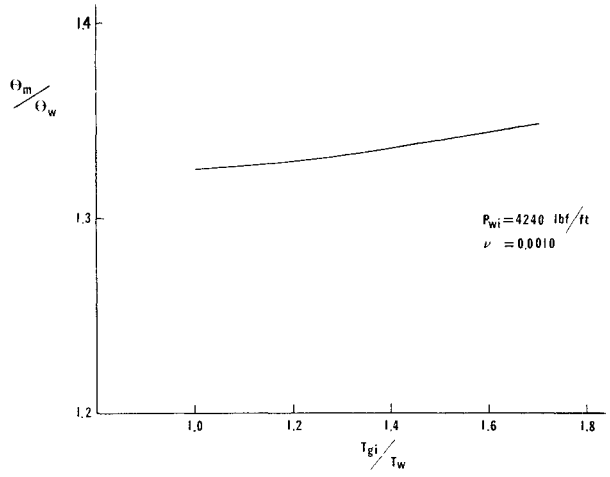

Fig. 8 Variation of thrust augmentation with air-injection temperature.

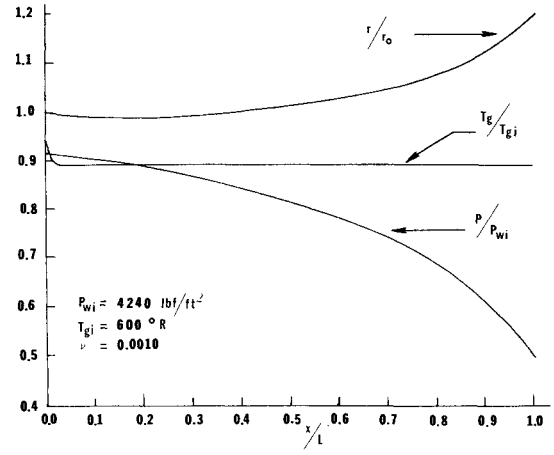

Fig. 10 Typical profiles of P, r, and T_g in two-phase nozzle flow.

lb/ft², a mass flow ratio of 0.0010, and various air-injection temperatures. An increase in the gas temperature of 70% results in a thrust increase of less than 2%. In Fig. 8 the ratio of augmented thrust to nonaugmented thrust is shown as a function of the ratio of air-inlet temperature to water temperature. Since the thrust is only weakly dependent on the air-injection temperature, it is concluded that the thermal energy of the higher-temperature air is lost by heat transfer to the water, which under the assumptions of the analysis acts as an infinite heat sink. The thrust increases noted are attributable to a small increase with increasing temperature in the void fraction at the mixing-chamber outlet.

The typical behavior of the nozzle flow parameters is illustrated in Fig. 9 and Fig. 10. For all conditions of temperature and pressure that are considered, the gas temperature falls to a value approximately equal to the water temperature within a nozzle distance of 5 bubble radii. The gas temperature remains essentially constant after its initially sharp decline.

Conclusions

It is concluded that for a specified water pump an air-augmented waterjet can be designed such that it produces a thrust in excess of that produced by the conventional waterjet. This method of thrust augmentation is especially attractive when considering water pumps which are incapable of delivering water at high pressures.

Thrust augmentation is only weakly dependent on air-injection temperature. Consequently, the air-augmented device can be designed for the temperature of the air most readily available without significant deviation from the maximum attainable thrust.

Increasing the mass flow ratio, within the range of values allowing bubbly flow, results in increased thrust augmentation.

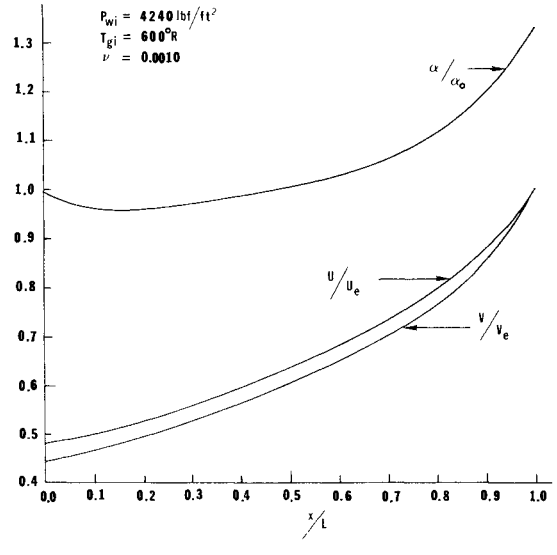

Fig. 9 Typical profiles of U, V, and α in two-phase nozzle flow.

References

[1]Taggart, R., "A Program for the Development of an Improved Hydraulic Jet Propulsion Device," *A.S.N.E. Journal*, Vol. 71, Nov. 1959, pp. 623–632.

[2]Berg, D. J., Jones, W. S., and Marron, H. W., "Why Waterjets?" *Naval Engineers Journal*, Vol. 79, Oct. 1967, pp. 779–782.

[3]Taggart, R., "Special Purpose Marine Propulsion Systems, Part II," *A.S.N.E. Journal*, Vol. 71, Nov. 1959, pp. 615–621.

[4]Muench, R. K. and Keith, T. G., "A Preliminary Parametric Study of a Water-Augmented Airjet for High-Speed Ship Propulsion," Rept. MEL 358/66, February 1967, Navy Marine Engineering Laboratory, Annapolis, Maryland.

[5]Smith, J. and Fox, R. M., "Reference Design Study of Mist-Jet Propulsion Systems in Captured-Air-Bubble Ships," Rept. NSRDC 2496, Nov. 1967, Naval Ship Research and Development Center, Washington, D.C.

[6]Hatte, R. and Davis, H. J., "Selection of Hydrofoil Waterjet Propulsion Systems," *Journal of Hydronautics*, Vol. 1, No. 1, July 1967, pp. 12–22.

[7]Johnson, V. E., Jr., "Water-Jet Propulsion for High-Speed Hydrofoil Craft," *Journal of Aircraft*, Vol. 3, No. 2, March-April 1966, pp. 174–179.

[8]Arcand, L. and Comolli, C. R., "Waterjet Propulsion for High-Speed Ships," Rept. PDS-2391, April 1967, Pratt and Whitney Aircraft Research and Development Center, West Palm Beach, Fla.

[9]Brandau, J. H., "Performance of Waterjet Propulsion Systems—A Review of the State-of-the-Art," *Journal of Hydronautics*, Vol. 2, No. 2, April 1968, pp. 61–73.

[10]Gasiunas, A. and Lewis, W. P., "Hydraulic Jet Propulsion: A Theoretical and Experimental Investigation into the Propulsion of Seacraft by Water Jets," *Proceedings of the Institution of Mechanical Engineers*, Vol. 78, Pt. 1, No. 7, 1963–64, pp. 185–200.

[11]DeLao, M., "Some Experimental Results of Tests of a Low-Speed, Waterjet Propulsion System," *Journal of Hydronautics*, Vol. 1, No. 2, Oct. 1967, pp. 97–101.

[12]Arcand, L. and Comolli, C. R., "Optimization of Waterjet Propulsion for High-Speed Ships," *Journal of Hydronautics*, Vol. 2, No. 1, Jan. 1968, pp. 2–8.

[13]"Waterjet Propulsion System Study. Report Number 2: Pump Selection and Design," Rept. LR 17885-2, 1965, Lockheed California Co., Burbank, Calif.

[14]"Waterjet Propulsion System Study. Report Number 3: Internal Flow Tests," Rept. LR 17885-3, 1965, Lockheed California Co., Burbank, Calif.

[15]"Waterjet Propulsion System Study. Report Number 5: System Design and Analysis," Rept. LR 17885-5, 1965, Lockheed California Co., Burbank, Calif.

[16]Wallis, G. B., *One-Dimensional Two-Phase Flow*, McGraw-Hill, New York, 1969, pp. 244–246.

[17]Hinze, J. O., "Fundamentals of the Hydrodynamic Mechanism of Splitting in Dispersion Processes," *A.I.Ch.E. Journal*, Vol. 1, No. 3, Sept. 1955, pp. 289–295.

[18]Tangren, R. F., Dodge, C. H., and Seifert, H. S., "Compressibility Effects in Two-Phase Flow," *Journal of Applied Physics*, Vol. 20, No. 7, July 1949, pp. 637–645.

[19]Mottard, E. J. and Shoemaker, C. J., "Preliminary Investigation of an Underwater Ramjet Powered by Compressed Air," TN D-991, Dec. 1961, NASA.

[20]Muir, J. F. and Eichhorn, R., "Compressible Flow of an Air-Water Mixture Through a Vertical, Two-Dimensional, Converging-Diverging Nozzle," *Proceedings of the 1963 Heat Transfer and Fluid Mechanics Institute*, Stanford University Press, Stanford, Calif. 1963, pp. 183–204.

[21]Witte, J. H., "Predicted Performance of Large Water Ramjets," unpublished work, Hydronautics, Inc., Laurel, Md., 1969.

[22]Vliet, G. C. and Leppert, G., "Forced Convection Heat Transfer from an Isothermal Sphere to Water," *Journal of Heat Transfer*, Vol. 83, May 1961, pp. 163–175.

[23]Sclichting, H., *Boundary Layer Theory*, McGraw-Hill, New York, 1968, p. 108.

[24]Bird, R. B., Stewart, W. E., and Lightfoot, E. N., *Transport Phenomena*, Wiley, New York, 1960, p. 192.

[25]Haberman, W. L. and Morton, R. K., "An Experimental Investigation in the Drag and Shape of Air Bubbles Rising in Various Liquids," D.T.M.B. Rept. 802, Sept. 1953, Dept. of the Navy, Washington, D.C.

[26]Gouse, S. W., Jr. and Brown, G. A., "A Survey of the Velocity of Sound in Two-Phase Mixtures," 64-WA/FE-35, Nov. 1965. American Society of Mechanical Engineers, New York.

[27]Henry, R. E., Grolmes, M. A., and Fauske, H. K., "Propagation Velocity of Pressure Waves in Gas-Liquid Mixtures," *Cocurrent Gas-Liquid Flow*, Plenum Press, New York, 1969, pp. 1–18.

[28]Kreyszig, E., *Advanced Engineering Mathematics*, Wiley, New York, 1962, pp. 92–94.

APRIL 1973 J. HYDRONAUTICS VOL. 7, NO. 2

Dynamic Response of Marine Propellers to Nonuniform Flowfields

Hideya Tsushima*
and
Maurice Sevik†
The Pennsylvania State University, University Park, Pa.

The necessity to reduce propeller-induced ship vibrations has led to the adoption of skewed blades. Such blades are more flexible than conventional ones and respond dynamically to the nonuniform velocity field generated by a ship's hull. The resulting time-dependent hydrodynamic and inertial loads may either alleviate or magnify the over-all forces and couples exerted by the propeller. These hydroelastic effects have been analyzed theoretically and verified experimentally on a model propeller.

Nomenclature

$A(\phi_\alpha,\bar{m})$ = integrand of lift operator
f = time-dependent load acting on a blade element
F = time-dependent hydrodynamic load due to nonuniform inflow velocity field
J = number of radial strips subdiving each blade
$K(\ )$ = kernel function of integral equation
$L(\ )$ = spanwise hydrodynamic load function
M_k = generalized mass corresponding to the kth mode of vibration
Δp = unsteady hydrodynamic pressure acting on the blade surface
P = hydrodynamic force due to dynamic response of the blades
q = order of blade harmonic
r_0 = tip radius of propeller
r_h = hub radius of propeller
s = width of radial strip
S = area of blade surfaces
t = time
U = volume mean velocity = $\dfrac{\int_0^{2\pi}\int_{r_h}^{r_0} V(r,\phi)r\,dr\,d\phi}{\pi(r_0^2 - r_h^2)}$
$V(r)$ = Fourier component of wake velocity normal to the blade
$w(X,r,\phi;t)$ = self-induced velocity at a control point at time t
X,r,ϕ = cylindrical coordinate system of control point
α_k,β_k = mode shape factors associated with the kth natural frequency
$\beta(r)$ = pitch angle of blade at radial position r
γ_q = phase angle of blade harmonic
$\delta(\rho,\theta;t)$ = deformation function of the blade at time t
$\Delta_k(\omega)$ = amplitude of the normal coordinates cooresponding to the kth mode of vibration
η = loss of factor of blade material
$\theta_b{}^r$ = projected propeller semichord length at radius r
ι = $(-1)^{1/2}$
ξ,ρ,θ = cylindrical coordinate system of loading point
Ξ_k = generalized force corresponding to the kth mode of vibration
$\xi_k(t)$ = normal coordinate associated with the kth mode of vibration
ρ_f,ρ_R = mass density of fluid and propeller blade material, respectively
σ^r = angular measure of skew at radius r
$\psi_k(\rho,\theta)$ = normalized mode shape of the blade corresponding to the kth natural frequency
ω = angular frequency
$(\cdot)$ = differentiation with respect to time

Subscripts
$(\ )$ = vector quantity, printed in boldface type
$(\ )_0$ = initial position of control point in propeller plane
$(\ )_\alpha$ = angular chordwise location of control point

Received August 7, 1972.
Index category: Propulsion System Hydrodynamics.

*Graduate Assistant, Department of Aerospace Engineering.

†Professor of Aerospace Engineering, and Director, The Garfield Thomas Water Tunnel; Ordnance Research Laboratory; presently Associate Technical Director, Naval Ship Research and Development Center, Carderock, Md. Associate Fellow AIAA.

Introduction

AN important problem in ship design concerns the vibrations generated by the propeller. Due to its response to a spatially and temporally nonuniform velocity field within